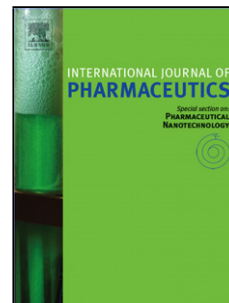


## Accepted Manuscript

Title: AC and DC electrospinning of hydroxypropylmethylcellulose with polyethylene oxides as secondary polymer for improved drug dissolution

Author: Attila Balogh Balázs Farkas Geert Verreck Jürgen Mensch Enikő Borbás Brigitta Nagy György Marosi Zsombor Kristóf Nagy



PII: S0378-5173(16)30224-1  
DOI: <http://dx.doi.org/doi:10.1016/j.ijpharm.2016.03.024>  
Reference: IJP 15622

To appear in: *International Journal of Pharmaceutics*

Received date: 5-2-2016  
Revised date: 14-3-2016  
Accepted date: 15-3-2016

Please cite this article as: Balogh, Attila, Farkas, Balázs, Verreck, Geert, Mensch, Jürgen, Borbás, Enikő, Nagy, Brigitta, Marosi, György, Nagy, Zsombor Kristóf, AC and DC electrospinning of hydroxypropylmethylcellulose with polyethylene oxides as secondary polymer for improved drug dissolution. *International Journal of Pharmaceutics* <http://dx.doi.org/10.1016/j.ijpharm.2016.03.024>

This is a PDF file of an unedited manuscript that has been accepted for publication. As a service to our customers we are providing this early version of the manuscript. The manuscript will undergo copyediting, typesetting, and review of the resulting proof before it is published in its final form. Please note that during the production process errors may be discovered which could affect the content, and all legal disclaimers that apply to the journal pertain.

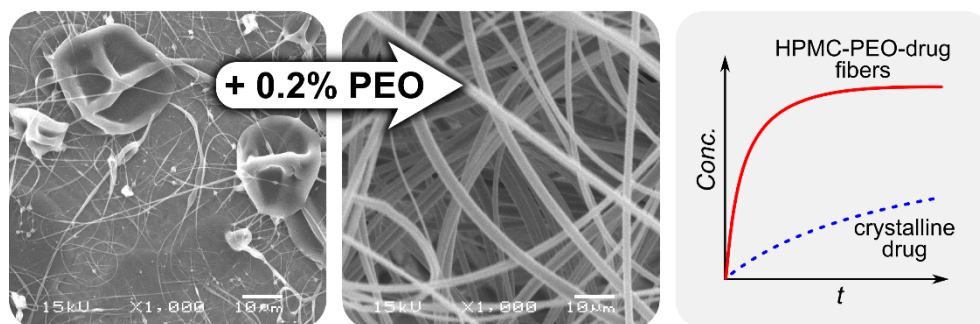
## **AC and DC electrospinning of hydroxypropylmethylcellulose with polyethylene oxides as secondary polymer for improved drug dissolution**

Attila Balogh<sup>1</sup>, Balázs Farkas<sup>1</sup>, Geert Verreck<sup>2</sup>, Jürgen Mensch<sup>2</sup>, Enikő Borbás<sup>1</sup>, Brigitta Nagy<sup>1</sup>, György Marosi<sup>1</sup>, Zsombor Kristóf Nagy<sup>1,\*</sup>

<sup>1</sup>Budapest University of Technology and Economics, Organic Chemistry and Technology Department, H-1111 Budapest, Hungary

<sup>2</sup>Chemical and Pharmaceutical Development, Johnson & Johnson Pharmaceutical Research and Development, Janssen Pharmaceutica, B-2340 Beerse, Belgium

\* Corresponding author. Tel.: +36-1-4631424; Fax: +36-1-4633648; E-mail: zsknagy@oct.bme.hu; Postal address: Hungary, 1111 Budapest, Budafoki út 8.

**GRAPHICAL ABSTRACT****AC/DC electrospinning of HPMC for dissolution improvement****ABSTRACT**

Alternating current electrospinning (ACES) capable to reach multiple times higher specific productivities than widely used direct current electrospinning (DCES) was investigated and compared with DCES to prepare drug-loaded formulations based on one of the most widespread polymeric matrix used for commercialized pharmaceutical solid dispersions, hydroxypropylmethylcellulose 2910 (HPMC). In order to improve the insufficient spinnability of HPMC (both with ACES and DCES) polyethylene oxide (PEO) as secondary polymer with intense ACES activity was introduced into the electrospinning solution. Different grades of this polymer used at as low concentrations in the fibers as 0.1% or less enabled the production of high quality HPMC-based fibrous mats without altering its physicochemical properties remarkably. Increasing concentrations of higher molecular weight PEOs led to the thickening of fibers from submicronic diameters to several microns of thickness. ACES fibers loaded with the poorly water-soluble model drug spironolactone were several times thinner than drug-loaded fibers prepared with DCES in spite of the higher feeding rates applied. The amorphous HPMC-based fibers with large surface area enhanced the dissolution of spironolactone significantly, the presence of small amounts of PEO did not affect the dissolution rate. The presented results confirm the diverse applicability of ACES, a novel technique to prepare fibrous drug delivery systems.

**Keywords: electrospinning; nanofibers; hypromellose; dissolution enhancement; polyethylene oxide**

**1. INTRODUCTION**

As a consequence of the increasing number of poorly water-soluble drugs in the recent decades numerous techniques have been developed to improve the dissolution properties, and thus, the bioavailability of these substances (Kawabata et al., 2011). Among other physical approaches such as nanosuspensions (Müller et al., 2001), crystallization techniques (Fages et al., 2004; Rasenack and Müller, 2002) and the use of solubilizers (e.g., surfactants (Lawrence and Rees, 2000; Pouton, 1997) and cyclodextrins (Brewster and Loftsson, 2007)), polymer-based solid dispersions has received a great deal of attention to overcome the hurdle of limited solubility (Vasconcelos et al., 2007). Amorphous solid dispersion of a drug in an inert water-soluble matrix (most often a polymer) ensure improved dissolution owing to three reasons: on the one hand higher solubility of the amorphous drug, on the other hand the well-soluble hydrophilic carrier used, thirdly an increased surface area can be obtained depending on the preparation method (Nagy et al., 2012). Accordingly, several amorphous solid dispersion-based products have been reached commercialization in the pharmaceutical market (Vaka et al., 2014).

Electrospinning (ES) is considered to be the simplest technique to produce ultrafine fibers with average diameters of 10 nm to 10  $\mu\text{m}$  from solution or melt (H. Wang et al., 2015) under the drawing force of the electrostatic field (Li and Xia, 2004; Reneker et al., 2007). Solvent-based electrospinning has been found to be an excellent method also for the preparation of solid dispersions due to the fast and, thus, very efficient amorphization of the drug enclosed in the fibers owing a large surface area (Sebe et al., 2015; Yu et al., 2009). Although various modifications have been published in respect to the ES setup related mostly to the spinneret (e.g., needleless (Molnár and Nagy, 2016), side-by-side (Yu et al., 2016) or multiaxial electrospinning (Illangakoon et al., 2015; X. Wang et al., 2015; Yang et al., 2016; Yu et al., 2015)), the challenge of increasing the productivity of ES could not have been addressed considering the high output of other fiber formation techniques such as melt blowing (Balogh et al., 2015b). Recent efforts for scaling up of ES combine the electrostatic field with another fiber formation force such as centrifugal force at low (Lomov and Molnár, 2015) and high (Nagy et al., 2015) frequencies, or a blow of air (Balogh et al., 2015c). However, as Pokorny and his coworkers have pointed out, replacing the static direct current (DC) high voltage source generally used for ES to a dynamic alternating current (AC) high voltage also results in a significant increase in productivity (Pokorny et al., 2014).

Alternating current electrospinning (ACES) provides a fairly different way of fiber generation than direct current electrospinning (DCES) which can be summarized as follows:

- Higher throughput rates than DCES. The multiple liquid jets ejected from the continuously charged-discharged droplet result in multiple-fold rise (up to 20-fold with the same spinneret) in productivities during ACES (Lawson et al., 2016; Pokorny et al., 2014).
- Collectorless operation. The movement of the flying AC electrospun so-called nanofibrous plume is not affected by ground potential, rather the electric wind surrounding the spinneret, i.e., there is no need for a grounded collector (Fig. 1). Assuming fiber production in a closed equipment (the case with pharmaceuticals), the collection is much easier if the sticking behavior of the fibers observable during DCES can be eliminated on grounded surfaces (i.e., almost every other part except the charged spinneret).
- Yarn production. Yarns are the building blocks of other 3-dimensional high value fibrous applications (e.g., tissue engineering, composites, etc.), however, preparing them using popular DCES is complicated due to the repulsion among the flying fibers (Sun et al., 2014). In contrast, the AC electrospun plume can readily turn into twisted yarns without difficult collection (Pokorny et al., 2014).
- Various influencing factors. Besides the main factors affecting DCES (e.g., polymer concentration, electric field strength, etc.), further possibilities arise such as variations in frequency and waveform of the AC voltage which can be presumably used to modify the ACES process (e.g., in respect of productivity or fiber morphology).

In our preceding work we demonstrated that ACES is also capable to produce drug-loaded fibrous fabrics based on of three pharmaceutically relevant polymers (Eudragit® E, Eudragit® L 100-55 and polyvinylpyrrolidone K90 (Balogh et al., 2015a)). Nevertheless, the majority (around 50%) of the amorphous solid dispersion-based pharmaceutical products commercially available is based on hydroxypropylmethylcellulose (hypromellose, HPMC) (Vo et al., 2013). HPMC is a water-soluble hydrophilic non-ionic cellulose ether generally used for controlled release tablets due to the polymeric gel layer formed when contacted with aqueous media (Li et al., 2005). The success of HPMC as the matrix of amorphous solid dispersions can be attributed to the following reasons: (1) HPMC has a high glass transition

temperature around 155°C (HPMC 2910 (Nyamweya and Hoag, 2000)) ensuring appropriate physical as well as chemical stability for the drug at storage temperature (Hancock et al., 1995). (2) The precipitation of the supersaturated drug in the dissolution media can be effectively inhibited with the use of HPMC (Brouwers et al., 2009). For instance, addition of small amount (5%) of HPMC into a surfactant-based formulation of poorly soluble paclitaxel resulted in a 10-fold increase in oral bioavailability in rats due to the precipitation inhibition effect (Gao and Morozowich, 2006).

Thus, in the work outlined in this paper we attempted to prepare electrospun HPMC-based fibers for drug delivery purposes for the first time using ACES, and compare ACES to DCES. However, the first results obtained left a lot to be desired due to the unacceptable morphology of electrospun HPMC. Therefore, based on our experience with ACES of high molecular weight polyethylene oxides (PEOs), compositions of HPMC combined with small amounts of PEOs were developed with a focus on increasing the throughput rate of ACES. The incorporation of a poorly water-soluble model drug (spironolactone) into the optimized HPMC-PEO compositions was then evaluated in respect to the effect of drug loading on fiber morphology, the physical state of the drug and *in vitro* dissolution, respectively.

## 2. MATERIALS AND METHODS

### 2.1. Materials

Spironolactone (SPIR) from Sigma-Aldrich (Budapest, Hungary) was used as API. Hydroxypropylmethylcellulose 2910 5 mPa·s (HPMC) was obtained from Aqualon, Hercules (Zwijndrecht, the Netherlands) where 5 mPa·s denotes the viscosity of the aqueous 2% (w/w) gel of HPMC (Li et al., 2005). Different grades of polyethylene oxide (PEO) (Mw=100 kDa (100kPEO), 1 MDa (1MPEO), 4 MDa (4MPEO)) were kindly provided by Colorcon (Budapest, Hungary). Absolute ethanol and dichloromethane was purchased from Molar Chemicals (Budapest, Hungary).

### 2.2. Direct current electrospinning (DCES)

The direct current solvent-based electrostatic spinner used in the experiments was equipped with NT-35 high voltage direct current supply (MA2000; Unitronik Ltd, Nagykanizsa, Hungary). The electrical potential applied on the spinneret electrode was 25 kV in all cases. A grounded aluminum plate covered with aluminum foil was used as collector. The distance of the spinneret and the collector was 20 cm and the experiments were performed at room temperature. Solutions of the polymeric excipients and the drug were prepared for electrospinning using a magnetic stirrer (600 rpm). The solutions were dosed by a SEP-10S Plus type syringe pump (Aitecs, Vilnius, Lithuania) through a needle spinneret (1 mm ID, 2 mm OD). Dosing rate of 10 mL/h was tested.

### 2.3. Alternating current electrospinning (ACES)

The alternating current electrospinning experiments were conducted using an FME-24 voltage transformer (24000 V/100 V ratio) (Transz vill Ltd, Budapest, Hungary) fed by a 0-230 V variable transformer. The electrical potential applied on the spinneret electrode was 25 kV (root mean square, RMS) at the frequency of the mains voltage (50 Hz). The sinusoidal AC high voltage was controlled by manual feedback using the variable transformer based on the measured output signal of a high voltage probe connected to the electrode. The preparation of polymer solutions was identical to that of used for DCES. The solutions were

dosed by a SEP-10S Plus type syringe pump through the same spinneret applied for DCES. Dosing rates of 10 mL/h and 30 mL/h were tested, respectively.

#### 2.4. Scanning electron microscopy (SEM) and fiber diameter analysis

Morphology of the samples was investigated by a JEOL 6380LVa (JEOL, Tokyo, Japan) type scanning electron microscope. Each specimen was fixed by conductive double-sided carbon adhesive tape and sputter-coated with gold prior to the examination. Applied accelerating voltage and working distance were 15-30 kV and 10 mm, respectively. A randomized fiber diameter determination method was used based on SEM imaging as described in our previous work (Balogh et al., 2015b),  $n=100$  measurements were made on each sample.

#### 2.5. Differential Scanning Calorimetry (DSC)

Differential scanning calorimetry measurements were carried out using a Setaram (Calure, France) DSC 92 apparatus (sample weight: ~10-15 mg, open aluminium pan, nitrogen flush). The temperature program consisted of an isothermal period, which lasted for 1 min at 25°C, with subsequent linear heating from 25°C to 260°C at the rate of 10°C/min. Purified indium standard was used to calibrate the instrument.

#### 2.6. X-ray powder diffraction (XRPD)

Powder X-ray diffraction patterns were recorded by a PANalytical X'pert Pro MDP X-ray diffractometer (Almelo, The Netherlands) using Cu-K $\alpha$  radiation (1.542 Å) and Ni filter. The applied voltage was 40 kV while the current was 30 mA. The untreated materials, a physical mixture composition and the fibrous samples were analyzed for angles  $2\theta$  between 4° and 42°.

#### 2.7. *In vitro* dissolution measurement

The dissolution studies were performed using a Pharmatest PTWS 600 dissolution tester (USP II apparatus (paddle); Hainburg, Germany). Samples equivalent to 25 mg of SPIR were added directly in the dissolution vessel containing 900 mL dissolution liquid (pH=6.8 100 mM phosphate buffer prepared according to USP). Electrospun samples were used for dissolution tests as spun. The temperature was maintained at  $37\pm 0.5^\circ\text{C}$  and stirred at 100 rpm. An on-line coupled Agilent 8453 UV-Vis spectrophotometer (Palo Alto, California) was used to measure the concentration of dissolved SPIR at a wavelength of 244 nm. Percentage of dissolution was readily calculated according to the calibration curves of SPIR due to the lack of absorption peaks of the applied excipients in this range.

### 3. RESULTS AND DISCUSSION

#### 3.1. AC and DC electrospinning of HPMC and PEOs

The first electrospinning experiments revealed that HPMC alone cannot be considered as a good fiber forming polymer as both AC and DC electrospinning produced large HPMC particles with a minor thin (around 0.5  $\mu\text{m}$ ) fibrous fraction (Fig. 2). See Table 1. for experimental conditions of pure HPMC, the concentration of HPMC was based on earlier research results (Verreck et al., 2003a). DCES of the HPMC solution yielded somewhat more fibers than ACES among many droplets, however, the morphology of the product was still not

acceptable. Variations in the composition of the electrospinning solution (i.e., the concentration of HPMC in  $\pm 50\%$  range) did not result in an improved mat quality. Thus, further investigations had to be carried out in order to obtain a fibrous HPMC fabric with large surface area enough for fast dissolving pharmaceutical applications.

Besides HPMC, different grades of PEOs were also tested with DCES and ACES. See Table 1. for experimental conditions of pure PEOs based on preliminary optimization. DCES was found to be capable to produce uniform PEO fibers with diameters around  $1\ \mu\text{m}$  regardless the molecular weight of the polymer (Fig. 2). In contrast to that, only AC electrospun fibers of 100 kDa PEO could be prepared with an average diameter three times of that of the DC electrospun 100kPEO fibers. The solution of the higher molecular weight PEOs (1 MDa or 4 MDa) instantly turned into multiple long liquid jets from the tip of the spinneret at lower dosing rates (10 mL/h) during ACES. Besides that, certain part of the solution was also removed from inside the spinneret making the process halting for several seconds until the solution was refilled again by the pump. Applying higher ACES dosing rates of these high molecular weight PEO solutions resulted in some undesired spattering of the liquid without the formation of observable fibrous strands. The uncommon inability for ACES fiber formation of 1MPEO and 4MPEO implies that PEO-based solutions are more sensitive to the AC voltage compared to DCES at the same effective voltage.

Nevertheless, the opposite electrospinning behavior of HPMC and PEO (too moderate versus too active) might compensate each other in a combined composition, therefore, the next step was to experimentally verify that assumption.

### 3.2. Optimization of HPMC-PEO electrospinning

The combination of the poorly electrospunable HPMC and the over-ACES-active PEO was expected to resolve the difficulties experienced during the electrospinning experiments. Moreover, new advantages might be gained with an improved HPMC-based electrospinning system such as the increased feeding rates available with the ACES process.

In order to obtain the desired good quality HPMC fibrous mats, systematic tests were carried out at fixed HPMC concentration (750 mg in 10 mL 50:50 V/V% ethanol-dichloromethane solvent mixture). Since the concentrations of the electrospinning solutions of pure HPMC and those of 1MPEO and 4MPEO distinctly differ (Table 1.) it was anticipated that only small amount of PEO is required to advance the fiber formation of HPMC. Gradual increase in PEO content was tested during ACES of HPMC, the feeding rate of ACES was set to 30 mL/h. As a rule of thumb, the investigated concentration range of each PEO could be decreased by one order of magnitude in the presence of HPMC as the molecular weight of selected PEOs increased. While addition of a few percent was required from 100kPEO, only  $\sim 0.1\text{-}0.5\%$  of 1MPEO or  $\sim 0.03\text{-}0.05\%$  4MPEO was sufficient to observe satisfying HPMC fibers. Note that these w/w% values are based on weight of the dissolved pure HPMC which was taken as 100%.

Below a certain PEO concentration no fiber formation occurred, only droplets left the spinneret and too high PEO concentrations resulted in visible liquid droplet content included in the plume. Thus, an optimum could be determined in all cases where fibers without droplets could be collected. As depicted in Figure 3, the increasing concentration of 1MPEO and 4MPEO resulted in increasing average ACES fiber diameters of a few microns, while fibers containing 100kPEO had diameters around 500 nm regardless the concentration of the secondary polymer. The scanning electron microscopic images of all optimum HPMC-PEO AC electrospun fibers can be also seen in Figure 3 (marked with letters a, b and c). See Table 2 for exact optimum compositions.

ACES feeding rates above 30 mL/h (e.g., 50 mL/h) also resulted in excellent looking fibrous plumes when processing the optimum HPMC-PEO solutions using a needle spinneret, however, with an emerging dried droplet (of 20-50  $\mu\text{m}$  diameter size) content. The almost two orders of magnitude lower absolute concentration of PEOs in their combined solutions with HPMC compared to the corresponding concentration of the pure PEO solutions (Table 1. and Table 2.) implies that secondary bonding of HPMC with PEO plays an important role in fiber formation. The use of 4MPEO was found to be the most challenging with ACES. If very small deviations from the optimum occurred it affected not only the fiber diameter but led to larger visible liquid droplets in the flying fibrous plume.

### 3.3. Effect of drug loading on the morphology of HPMC-based AC and DC electrospun fibers

Spironolactone as poorly water-soluble model drug was incorporated into the optimized HPMC-based matrices as AC and DC electrospun fibers, the morphology of those can be seen in Figure 4.

Without PEO secondary polymer the 20% SPIR-loaded DC electrospun product contained mostly large droplets (10-50  $\mu\text{m}$  in size), however, the HPMC+40%SPIR composition processed with DCES was a more acceptable fibrous mat even if frequent defects such as droplets or large beads occurred. It can thus be concluded that the drug-loading has an improving effect on the quality of the electrospun HPMC-based fibers. That observation also explains why other research results present good quality DC electrospun HPMC fibers with itraconazole incorporated (Verreck et al., 2003a), presumably itraconazole aids similarly or even better the formation of HPMC fibers than SPIR.

AC electrospinning was used to prepare HPMC-PEO-SPIR fibers based on the optimized compositions and exploiting the elevated feeding rates available. Excellent morphology of the HPMC-PEO ACES SPIR-loaded fibers was achievable regardless the applied higher throughput rate. However, as an interesting side effect the reduction in average fiber diameter could be observed during ACES along with increasing SPIR loading. Our former experience with DC electrospun SPIR-loaded fibers showed that addition of the drug at relatively low ratio ( $\leq 20\%$ ) led to detectable thickening compared to the placebo nonionic Soluplus® fibers (Nagy et al., 2012). In order to explore the observed diameter reducing effect of ACES, the SPIR-loaded optimized HPMC-PEO fibers were also prepared with DCES applying a necessarily lower feeding rate (10 mL/h) and the same voltage as during ACES (25 kV DC).

The results of the fiber diameter evaluation of AC and DC electrospun HPMC-PEO fibers are shown in Figure 5. As it can be seen, DC electrospun fibers had larger average diameters in all cases regardless the molecular weight of the PEO or the ratio of the incorporated drug. This way the different effect of drug loading on the diameter of AC and DC electrospun fibers was confirmed. When 1MPEO or 4MPEO was used as secondary polymer, the DC electrospun SPIR-loaded fibers were several microns in thickness, while the average diameters of AC electrospun fibers with the same composition approached the submicronic region. In turn, using 100kPEO led to no significant thinning in the case of ACES regardless the drug loading (fibers were around 500 nm) and only negligible thickening (from 650 nm to 850 nm) could be detected without SPIR or with 40% SPIR incorporated into DC electrospun HPMC-100kPEO fibers.

It is worth to mention that the observed phenomenon described above may occur only when an ionic interaction is not present between the drug and the polymer or the solvent, respectively (which is the case with the HPMC-PEO-SPIR system). The experimental results with DC electrospinning of aqueous poly(vinyl alcohol) solutions revealed that the presence of drug has a thickening effect on the fiber diameter only if the drug was less ionizable (Taepaiboon et al., 2006). Furthermore, our recent results with ACES showed that electrospinning of a solution containing a weak base drug and an anionic polymer led to 4-6



times thicker fibers than the placebo electrospun polymer regardless the type of voltage (AC or DC) (Balogh et al., 2015a). The main reason of the different AC and DC electrospinning behavior of the same HPMC-PEO-SPIR solutions may lie in the different viscoelastic properties of the polymer liquid when an oscillating (ACES) or a constant (DCES) shear force is applied, therefore, more detailed studies are needed to elucidate the mechanisms of the observed effects.

### 3.4. Physical characterization of drug-loaded HPMC-based fibers

Physical state of SPIR in the HPMC-based fibrous solid dispersions was investigated using differential scanning calorimetry (DSC) and X-ray powder diffraction (XRPD) to determine the degree of crystallinity of the incorporated drug (Fig. 6). Both AC and DC electrospinning can be considered as a very effective tool to produce amorphous solid dispersions (solid solutions), however, the solubility advantage during dissolution can be exploited only if there are no crystalline traces of the drug in the formulation (Szabó et al., 2015).

The DSC thermogram of SPIR shows the melting peak of the crystalline structure at 213°C, while the melting of different grades of semi-crystalline PEOs occurs at regressively increasing temperatures as a function of molecular weight (65-70°C). In the case of a HPMC+5%SPIR physical mixture reference, besides the wide water loss below 100°C belonging to the hydrophilic HPMC polymer the melting of the crystalline drug could be also clearly detected. In contrast, the weak glass transition of HPMC was barely observable, the literature value for the glass transition temperature of HPMC 2910 is around 155°C (Nyamweya and Hoag, 2000). Accordingly, the lack of the crystalline SPIR related melting peak at around 210°C implies that both AC and DC electrospinning converted the drug into an amorphous form. Even if the DCES process of HPMC+SPIR compositions yielded products with imperfect quality (Fig. 4), the low feeding rate and highly volatile organic solvents allowed quick drying of the larger particles, and thus, amorphization of SPIR. A very low portion was used from the secondary polymer PEO in the HPMC-PEO-SPIR dispersions, however, the high enthalpy of fusion of PEOs might enable the detection of crystalline traces. Despite that, no endothermic peak could be measured at the melting point of different PEOs presumably due to their well-mixed state in the HPMC matrix.

Similarly to DSC, XRPD was also found to be very sensitive to the presence of crystalline structures. Crystalline SPIR as well as PEOs with different molecular weight displayed a series of characteristic sharp diffraction peaks when examined with XRPD. In the case of the physical mixture of HPMC+5%SPIR, the most intense peaks of SPIR were still observable and a weak sign of organized structure of HPMC also emerged at  $2\Theta=32^\circ$  which latter was confirmed by earlier studies as well (Verreck et al., 2003b). Bearing in mind all these and considering that SPIR is a poor glass former meaning that it rather tends to crystallize or remain crystalline than form amorphous clusters (Nagy et al., 2012), the absence of any X-ray diffraction phenomenon or endothermic melting peaks signifies a mixed amorphous form of all components including SPIR in the HPMC-based solid dispersions.

### 3.5. *In vitro* dissolution of drug-loaded HPMC-based fibers

The results of *in vitro* dissolution testing of the SPIR-loaded HPMC-based AC and DC electrospun fibers are presented in Fig. 7.

As it can be seen, crystalline SPIR dissolved very slowly, two hours were needed to exceed 50% dissolution. The electrospun fibers exhibited a significantly improved dissolution due to the large surface area and the increased solubility of the amorphous form of SPIR evidenced by DSC and XRPD. Theoretically, fibers with higher loadings of a poorly water-soluble drug

dissolve slower due to the hydrophobization effect of the drug on the hydrophilic carrier (Van Drooge et al., 2006). Despite that, HPMC-PEO+40%SPIR AC electrospun fibers dissolved almost two times faster than those of with 20% SPIR content. The reason behind that is the propensity of HPMC to form gels instead of dissolving. That way a fibrous structure quickly merges when contacted with water losing the large surface area, however, this phenomenon is hampered if the dispersion is more hydrophobic. Another peculiar behavior is that the HPMC+20%SPIR DCES product consisting mostly large droplets (Fig. 4) dissolved similarly than the good quality HPMC-PEO+20%SPIR ACES fibers. The HPMC+40%SPIR DCES fibers with a somewhat improved fibrous morphology dissolved noticeably slower than the AC electrospun HPMC-PEO fibers with the same fraction of SPIR. Although PEOs are known to have limited water solubility due to the very high molecular weights, using them as secondary polymers in low concentrations - similarly to the multiple times higher feeding rates of ACES - did not have notable effect on the dissolution characteristics. Overall, these observations suggest that the main determining factor of dissolution rate in the presented case is the ratio of the main ingredients, i.e., HPMC and SPIR but not PEO. Furthermore, other effects such as the diffusion of the active species out of the fibers may also occurred positively influencing the release rate (Russo and Lamberti, 2011). Higher specific surface area (Table 2.) became significant only if the aforementioned gelling is sufficiently suppressed like in the case of samples with 40% SPIR. However, the differences in specific surface area hardly affected the dissolution speed of those 40%SPIR AC electrospun fibers.

#### 4. CONCLUSIONS

Being one of the mostly used polymers for commercialized amorphous solid dispersion products, HPMC 2910 was processed with AC as well as DC electrospinning to improve the dissolution of a poorly water-soluble model drug, spironolactone. The insufficient morphology of electrospun HPMC was resolved by incorporating small amounts of PEO as secondary polymer overly sensitive to ACES. The use of lower grades of PEO such as 100 kDa and 1 MDa yielded good quality HPMC-based fibers. When PEO with molecular weight of 4 MDa was applied the fiber formation was more sensitive to small variations in secondary polymer concentration. No traces of crystallinity could be detected in the prepared fibers when conducting DSC and XRPD measurements, presumably SPIR and PEO turned into an amorphous form as a result of processing. Accordingly, the dissolution of SPIR could be greatly enhanced regardless the use of PEOs due to the large surface area, the hydrophilic HPMC carrier and the amorphous SPIR content of the fibers.

The main benefit of alternating current electrospinning, i.e., the multiple times higher feeding rates compared to regular direct current electrospinning, was also attainable during the production of HPMC-based fibers without remarkable deviations in morphology and physical state of the incorporated drug. Besides elevated feeding rates, an unexpected effect of alternating current electrospinning was observed: increasing fraction of SPIR resulted in thinner fibers as opposed to DCES of the same solutions. The exploration of alternating current electrospinning may be an important milestone on the way towards the industrial production of electrospun amorphous pharmaceutical solids, however, more detailed studies are still required to elucidate the mechanisms affecting ACES fiber formation.

#### 5. ACKNOWLEDGMENTS

We thank János Madarász for his excellent support in the XRPD measurements. This project was supported by the New Széchenyi Plan (project ID: TÁMOP-4.2.1/B-09/1/KMR-

2010-0002), OTKA grants PD-108975 and 112644, and the János Bolyai Research Scholarship of the Hungarian Academy of Sciences.

## 6. REFERENCES

- Balogh, A., Cselkó, R., Démuth, B., Verreck, G., Mensch, J., Marosi, G., Nagy, Z.K., 2015a. Alternating current electrospinning for preparation of fibrous drug delivery systems. *Int. J. Pharm.* 495, 75–80.
- Balogh, A., Farkas, B., Faragó, K., Farkas, A., Wagner, I., Van Assche, I., Verreck, G., Nagy, Z.K., Marosi, G., 2015b. Melt-blown and electrospun drug-loaded polymer fiber mats for dissolution enhancement : A comparative study. *J. Pharm. Sci.* 104, 1767–1776.
- Balogh, A., Horváthová, T., Fülöp, Z., Loftsson, T., Harasztos, A.H., Marosi, G., Nagy, Z.K., 2015c. Electroblowing and electrospinning of fibrous diclofenac sodium-cyclodextrin complex-based reconstitution injection. *J. Drug Deliv. Sci. Technol.* 26, 28–34.
- Brewster, M.E., Loftsson, T., 2007. Cyclodextrins as pharmaceutical solubilizers. *Adv. Drug Deliv. Rev.* 59, 645–66.
- Brouwers, J., Brewster, M.E., Augustijns, P., 2009. Supersaturating drug delivery systems : The answer to solubility-limited oral bioavailability? *J. Pharm. Sci.* 98, 2549–2572.
- Fages, J., Lochard, H., Letourneau, J.-J., Sauceau, M., Rodier, E., 2004. Particle generation for pharmaceutical applications using supercritical fluid technology. *Powder Technol.* 141, 219–226.
- Gao, P., Morozowich, W., 2006. Development of supersaturatable self-emulsifying drug delivery system formulations for improving the oral absorption of poorly soluble drugs. *Expert Opin. Drug Deliv.* 3, 97–110.
- Hancock, B.C., Shamblin, S.L., Zografi, G., 1995. Molecular mobility of amorphous pharmaceutical solids below their glass transition temperatures. *Pharm. Res.* 12, 799–806.
- Illangakoon, U.E., Yu, D.-G., Ahmad, B.S., Chatterton, N.P., Williams, G.R., 2015. 5-fluorouracil loaded Eudragit fibers prepared by electrospinning. *Int. J. Pharm.* 495, 895–902.
- Kawabata, Y., Wada, K., Nakatani, M., Yamada, S., Onoue, S., 2011. Formulation design for poorly water-soluble drugs based on biopharmaceutics classification system: basic approaches and practical applications. *Int. J. Pharm.* 420, 1–10.
- Lawrence, M.J., Rees, G.D., 2000. Microemulsion-based media as novel drug delivery systems. *Adv. Drug Deliv. Rev.* 45, 89–121.
- Lawson, C., Stanishevsky, A., Sivan, M., Pokorny, P., Lukáš, D., 2016. Rapid fabrication of poly (ε-caprolactone) nanofibers using needleless alternating current electrospinning. *J. Appl. Polym. Sci.* 133, [Epub ahead of print].

- Li, C.L., Martini, L.G., Ford, J.L., Roberts, M., 2005. The use of hypromellose in oral drug delivery. *J. Pharm. Pharmacol.* 57, 533–546.
- Li, D., Xia, Y., 2004. Electrospinning of nanofibers: Reinventing the wheel? *Adv. Mater.* 16, 1151–1170.
- Lomov, S. V., Molnár, K., 2015. Compressibility of carbon fabrics with needleless electrospun PAN nanofibrous interleaves. *Express Polym. Lett.* 10, 25–35.
- Molnár, K., Nagy, Z.K., 2016. Corona-electrospinning: Needleless method for high-throughput continuous nanofiber production. *Eur. Polym. J.* 74, 279–286.
- Müller, R.H., Jacobs, C., Kayser, O., 2001. Nanosuspensions as particulate drug formulations in therapy: Rationale for development and what we can expect for the future. *Adv. Drug Deliv. Rev.* 47, 3–19.
- Nagy, Z.K., Balogh, A., Démuth, B., Pataki, H., Vigh, T., Szabó, B., Molnár, K., Schmidt, B.T., Horák, P., Marosi, G., Verreck, G., Van Assche, I., Brewster, M.E., 2015. High speed electrospinning for scaled-up production of amorphous solid dispersion of itraconazole. *Int. J. Pharm.* 480, 137–142.
- Nagy, Z.K., Balogh, A., Vajna, B., Farkas, A., Patyi, G., Kramarics, Á., Marosi, G., 2012. Comparison of electrospun and extruded Soluplus®-based solid dosage forms of improved dissolution. *J. Pharm. Sci.* 101, 322–332.
- Nyamweya, N., Hoag, S.W., 2000. Assessment of polymer-polymer interactions in blends of HPMC and film forming polymers by modulated temperature differential scanning calorimetry. *Pharm. Res.* 17, 625–631.
- Pokorny, P., Kostakova, E., Sanetnik, F., Mikes, P., Chvojka, J., Kalous, T., Bilek, M., Pejchar, K., Valtera, J., Lukas, D., 2014. Effective AC needleless and collectorless electrospinning for yarn production. *Phys. Chem. Chem. Phys.* 16, 26816–26822.
- Pouton, C.W., 1997. Formulation of self-emulsifying drug delivery systems. *Adv. Drug Deliv. Rev.* 25, 47–58.
- Rasenack, N., Müller, B.W., 2002. Dissolution rate enhancement by in situ micronization of poorly water-soluble drugs. *Pharm. Res.* 19, 1894–1900.
- Reneker, D.H., Yarin, A.L., Zussman, E., Xu, H., 2007. Electrospinning of nanofibers from polymer solutions and melts. *Adv. Appl. Mech.* 41, 43–346.
- Russo, G., Lamberti, G., 2011. Electrospinning of drug-loaded polymer systems: Preparation and drug release. *J. Appl. Polym. Sci.* 122, 3551–3556.
- Sebe, I., Szabó, P., Kállai-Szabó, B., Zelkó, R., 2015. Incorporating small molecules or biologics into nanofibers for optimized drug release: A review. *Int. J. Pharm.* 494, 516–530.
- Sun, B., Long, Y.Z., Zhang, H.D., Li, M.M., Duvail, J.L., Jiang, X.Y., Yin, H.L., 2014. Advances in three-dimensional nanofibrous macrostructures via electrospinning. *Prog.*

- Polym. Sci. 39, 862–890.
- Szabó, P., Sebe, I., Stiedl, B., Kállai-Szabó, B., Zelkó, R., 2015. Tracking of crystalline-amorphous transition of carvedilol in rotary spun microfibers and their formulation to orodispersible tablets for in vitro dissolution enhancement. *J. Pharm. Biomed. Anal.* 115, 359–367.
- Taepaiboon, P., Rungsardthong, U., Supaphol, P., 2006. Drug-loaded electrospun mats of poly(vinyl alcohol) fibres and their release characteristics of four model drugs. *Nanotechnology* 17, 2317–2329.
- Vaka, S.R.K., Bommana, M.M., Desai, D., Djordjevic, J., Phuapradit, W., Shah, N., 2014. Excipients for amorphous solid dispersions, in: *Amorphous Solid Dispersions*. pp. 123–161.
- Van Drooge, D.J., Hinrichs, W.L.J., Visser, M.R., Frijlink, H.W., 2006. Characterization of the molecular distribution of drugs in glassy solid dispersions at the nano-meter scale, using differential scanning calorimetry and gravimetric water vapour sorption techniques. *Int. J. Pharm.* 310, 220–229.
- Vasconcelos, T., Sarmiento, B., Costa, P., 2007. Solid dispersions as strategy to improve oral bioavailability of poor water soluble drugs. *Drug Discov. Today* 12, 1068–1075.
- Verreck, G., Chun, I., Peeters, J., Rosenblatt, J., Brewster, M.E., 2003a. Preparation and characterization of nanofibers containing amorphous drug dispersions generated by electrostatic spinning. *Pharm. Res.* 20, 810–817.
- Verreck, G., Six, K., Mooter, G. Van Den, Peeters, J., Brewster, M.E., Van den Mooter, G., Baert, L., Peeters, J., Brewster, M.E., 2003b. Characterization of solid dispersions of itraconazole and hydroxypropylmethylcellulose prepared by melt extrusion - part I. *Int. J. Pharm.* 251, 165–174.
- Vo, C.L.-N., Park, C., Lee, B.-J., 2013. Current trends and future perspectives of solid dispersions containing poorly water-soluble drugs. *Eur. J. Pharm. Biopharm.* 85, 799–813.
- Wang, H., Xu, Y., Wei, Q., 2015. Preparation of bamboo-hat-shaped deposition of a poly(ethylene terephthalate) fiber web by melt-electrospinning. *Text. Res. J.* 85, 1838–1848.
- Wang, X., Yu, D.-G., Li, X.-Y., Bligh, S.W.A., Williams, G.R., 2015. Electrospun medicated shellac nanofibers for colon-targeted drug delivery. *Int. J. Pharm.* 490, 384–390.
- Yang, C., Yu, D.-G., Pan, D., Liu, X.-K., Wang, X., Bligh, S.W.A., Williams, G.R., 2016. Electrospun pH-sensitive core-shell polymer nanocomposites fabricated using a tri-axial process. *Acta Biomater.* [Epub ahead of print].
- Yu, D.-G., Li, X., Wang, X., Yang, J., Bligh, S.W.A., Williams, G.R., 2015. Nanofibers fabricated using triaxial electrospinning as zero order drug delivery systems. *ACS Appl.*

Mater. Interfaces 7, 18891–18897.

Yu, D.-G., Yang, C., Jin, M., Williams, G.R., Zou, H., Wang, X., Bligh, S.W.A., 2016. Medicated Janus fibers fabricated using a Teflon-coated side-by-side spinneret. *Colloids Surfaces B Biointerfaces* 138, 110–116.

Yu, D.-G., Zhu, L.-M., White, K., Brandford-White, C., 2009. Electrospun nanofiber-based drug delivery systems. *Health* 1, 67–75.



Figure 1. The nanofibrous plume generated during alternating current electrospinning without using a grounded collector (normal photographic image).

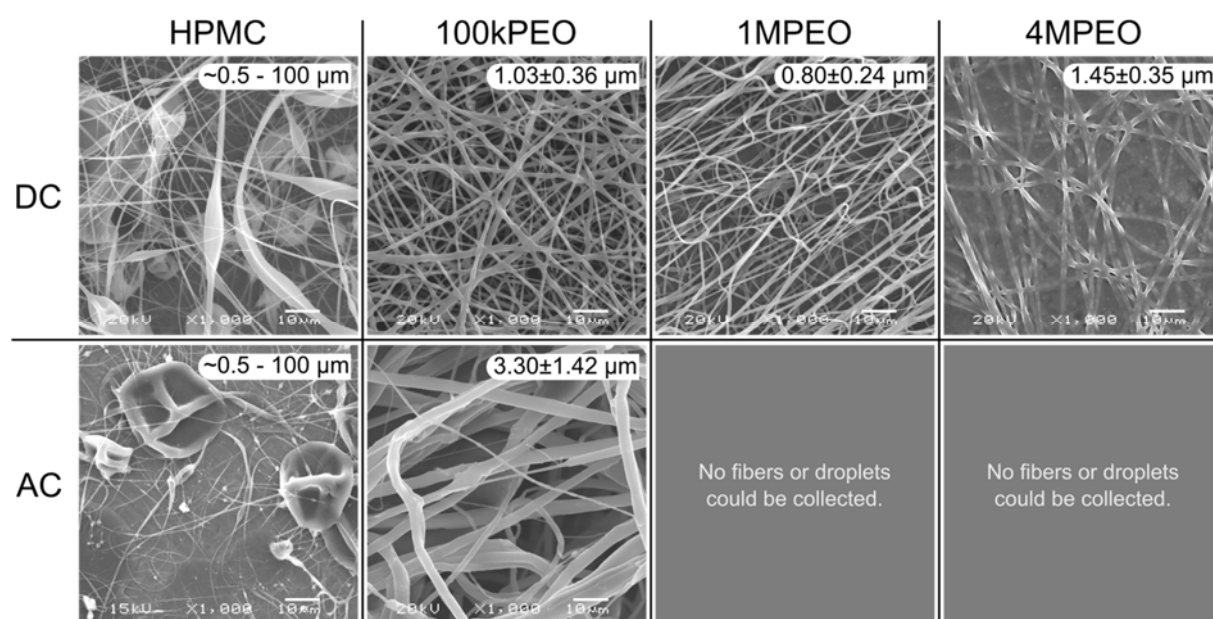
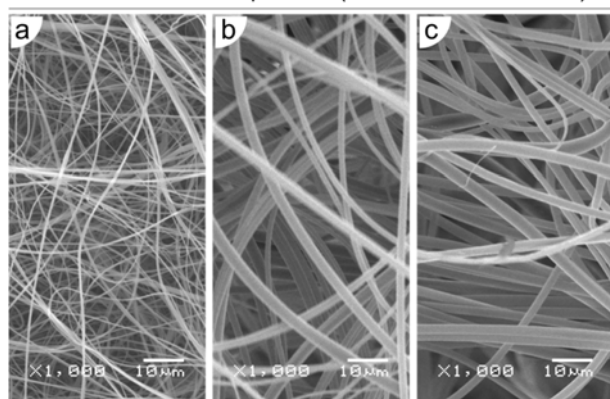
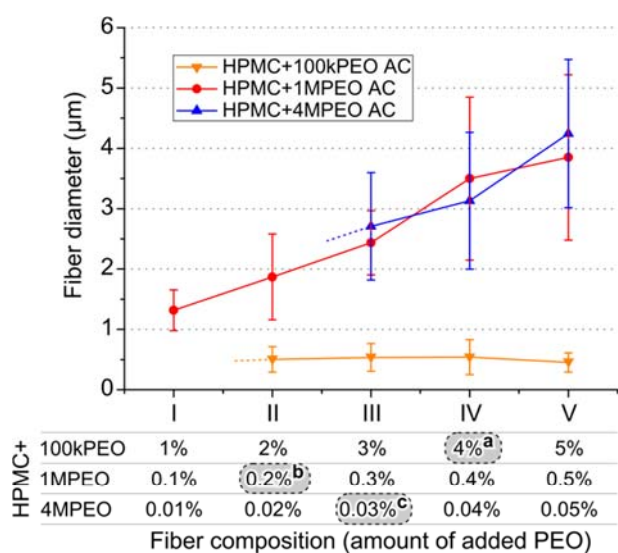


Figure 2. Scanning electron microscopic images of AC and DC electrospun hydroxypropylmethylcellulose 2910 (HPMC) and different grades of polyethylene oxides (100 kDa (100kPEO), 1 MDa (1MPEO), 4 MDa (4MPEO)).



**Figure 3.** Average fiber diameters of AC electrospun HPMC-based fibers as a function of amount of added PEO with different molecular weight (30 mL/h, 25 kV<sub>RMS</sub>). Letters (a), (b) and (c) mark the optimum compositions (see text and Table 2) and also the corresponding scanning electron microscopic images for each HPMC-PEO combination.



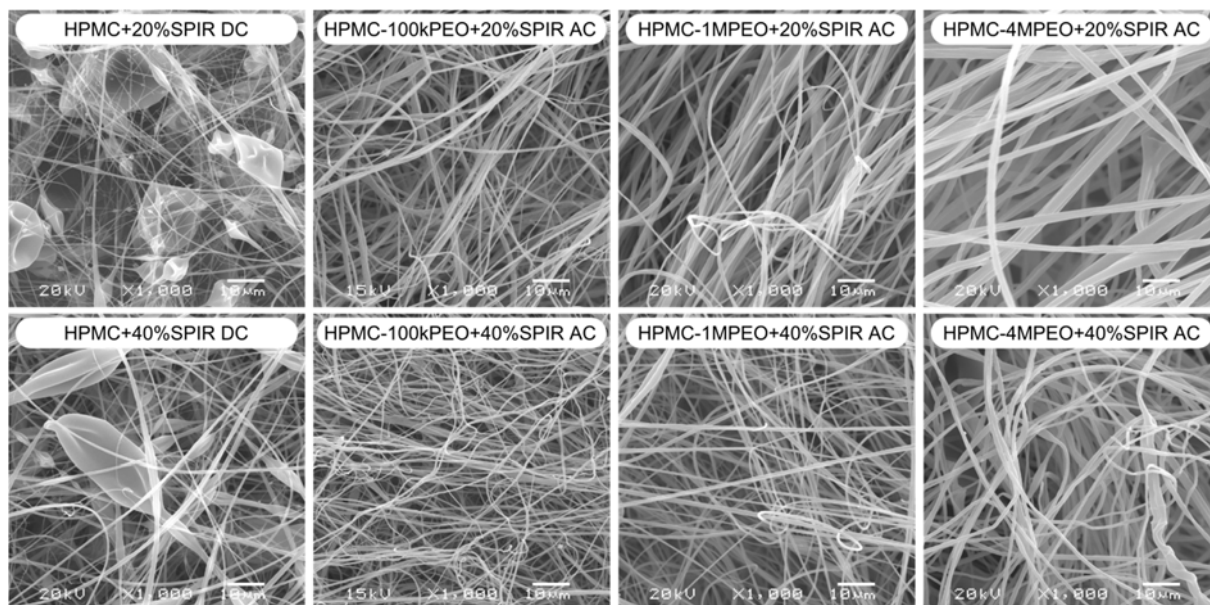


Figure 4. Scanning electron microscopic images of AC and DC electrospun spirinolactone-loaded (SPIR) HPMC-based fibers (DCES: 10 mL/h, 25 kV; ACES: 30 mL/h, 25 kV<sub>RMS</sub>).

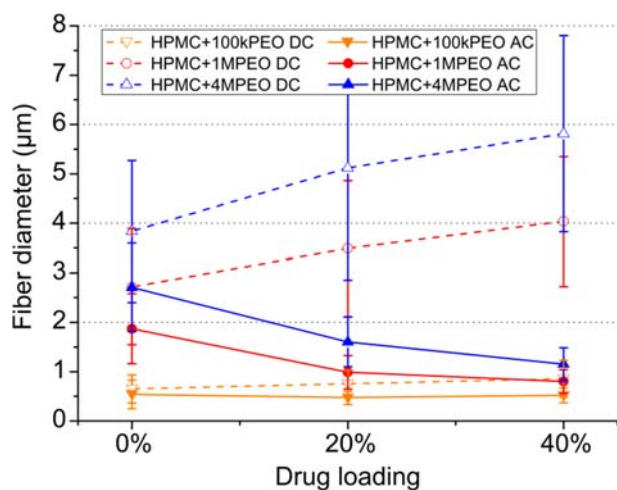
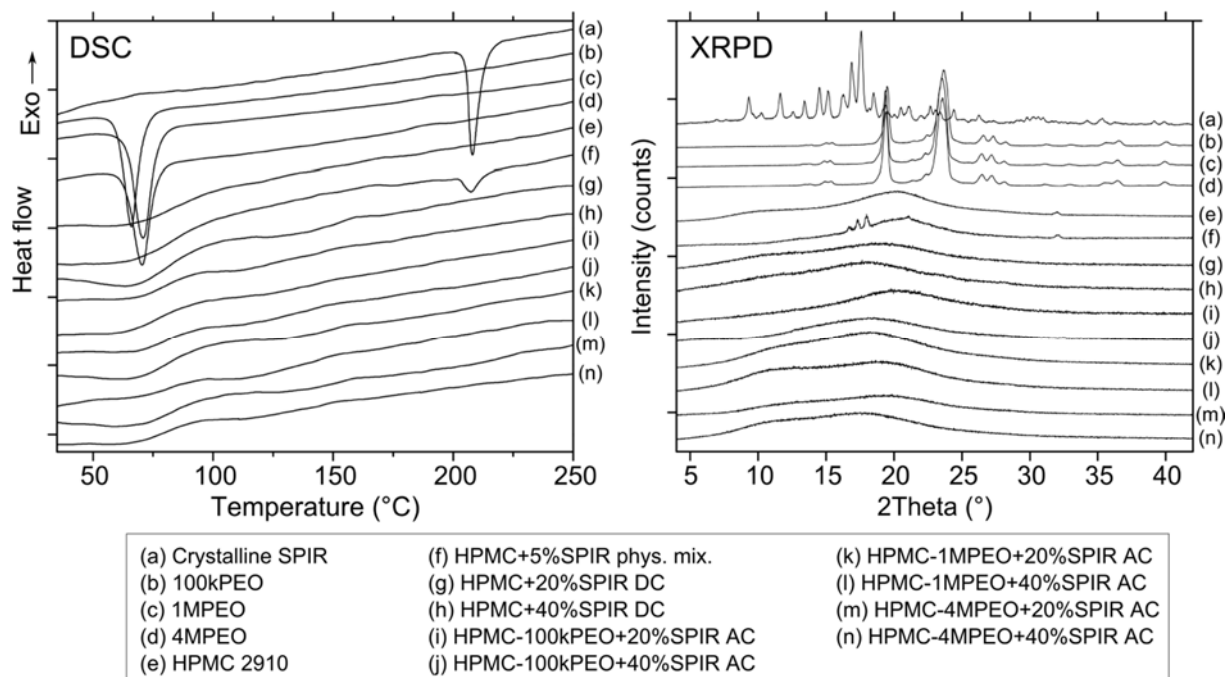
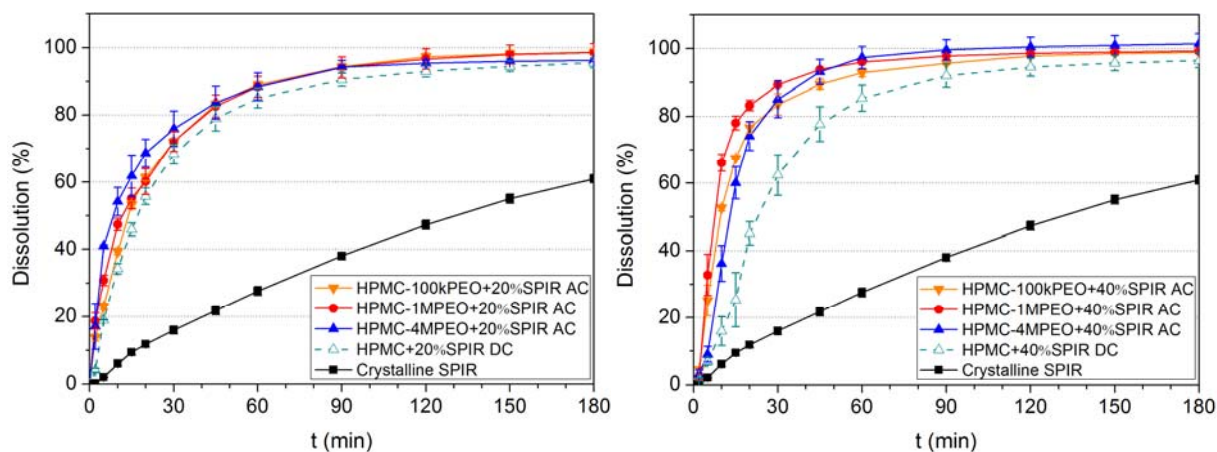


Figure 5. Average fiber diameters of different AC and DC electrospun HPMC-PEO fibers as a function of the amount of the incorporated drug (spirinolactone) (DCES: 10 mL/h, 25 kV; ACES: 30 mL/h, 25 kV<sub>RMS</sub>).



**Figure 6.** Differential scanning calorimetry thermograms (DSC) and X-ray powder diffraction patterns (XRPD) of (a) crystalline spirinolactone (SPIR), (b-d) applied grades of polyethylene oxides (PEO), (e) hydroxypropylmethylcellulose 2910 (HPMC), (f) physical mixture of HPMC and 5% SPIR, and (g-n) AC and DC electrospun HPMC-based SPIR-loaded fibers.



**Figure 7.** Dissolution profiles of SPIR from drug-loaded HPMC-based AC and DC electrospun fibers (as spun) containing 20% (left) or 40% (right) SPIR. The error bars indicate the standard deviations ( $n=3$ ). [25 mg dose, 900 mL pH=6.8 100 mM phosphate buffer, USP Dissolution Apparatus 2 (paddle), 100 rpm, 37°C]

**Table 1. AC and DC electrospinning parameters of hydroxypropylmethylcellulose 2910 (HPMC) and different grades of polyethylene oxides (100 kDa (100kPEO), 1 MDa (1MPEO), 4 MDa (4MPEO)). Applied voltage and feeding rate were 25 kV<sub>RMS</sub> and 10 mL/h, respectively.**

Polymer	Dissolved polymer in 10 mL ethanol-dichloromethane (50:50 V/V%) (mg)
HPMC	750
100kPEO	875
1MPEO	37.5
4MPEO	10.6

**Table 2. AC and DC electrospinning parameters and specific surface area of hydroxypropylmethylcellulose 2910 (HPMC)-based dispersions without or with optimized amount of different grades of polyethylene oxides (100 kDa (100kPEO), 1 MDa (1MPEO), 4 MDa (4MPEO)), and spirinolactone (SPIR), respectively. Applied voltage was 25 kV<sub>RMS</sub> in all cases, DCES and ACES feeding rates were fixed to 10 and 30 mL/h, respectively.**

Sample	Dissolved amount in 10 mL ethanol-dichloromethane (50:50 V/V%) (mg)			Specific surface area (m <sup>2</sup> /g) <sup>a</sup>
	HPMC	PEO	SPIR	
HPMC+4%100kPEO	750	30	0	5,8
HPMC+0.2%1MPEO	750	1.5	0	1,7
HPMC+0.03%4MPEO	750	0.23	0	1,2
HPMC+20%SPIR <sup>b</sup>	750	0	188	-
HPMC+40%SPIR <sup>b</sup>	750	0	500	-
HPMC-100kPEO+20%SPIR	750	30	195	6,2
HPMC-100kPEO+40%SPIR	750	30	520	6,0
HPMC-1MPEO+20%SPIR	750	1.5	188	3,2
HPMC-1MPEO+40%SPIR	750	1.5	500	3,9
HPMC-4MPEO+20%SPIR	750	0.23	188	1,9
HPMC-4MPEO+40%SPIR	750	0.23	500	2,7

<sup>a</sup> Estimated based on SEM images (density of HPMC = 1280 kg/m<sup>3</sup>)

<sup>b</sup> Only DC electrospun poor quality samples (see Fig 4.) were prepared, specific surface area is not calculated